Dalton Transactions

COMMUNICATION

Cite this: *Dalton Trans.*, 2020, **49**, 274

Received 8th November 2019, Accepted 26th November 2019

DOI: 10.1039/c9dt04327f

rsc.li/dalton

# Direct conversion of uranium dioxide $UO_2$ to uranium tetrafluoride $UF_4$ using the fluorinated ionic liquid [Bmim][$PF_6$]†

Florian Joly,[a] Pardis Simon,[a] Xavier Trivelli,[b] Mehdi Arab,[c] Bertrand Morel,[c] Pier Lorenzo Solari,[d] Jean-Francois Paul,[a] Philippe Moisy[e] and Christophe Volkringer *[a,f]

**The industrial fluorination of $UO_2$ to $UF_4$ is based on a complex process involving the manipulation of a large amount of HF, a very toxic and corrosive gas. We present here a safer way to accomplish this reaction utilizing ionic liquid [Bmim][$PF_6$] as a unique reaction medium and fluoride source.**

Uranium is the main component of nuclear fuel and is used for the production of energy.[1] After its extraction from natural ores and purification, this element is transformed into stable oxides $UO_3$ or $U_3O_8$, before further operations. To produce nuclear fuel, these oxides are usually reduced in order to generate $UO_2$. This compound is well adapted to the fluorination of uranium during a process called conversion.[2] During this essential step, uranium is first precipitated as uranium tetrafluoride $UF_4$ by hydrofluorination. This solid can be stored under anhydrous conditions or converted into gaseous $UF_6$. This last species is the main reagent for uranium enrichment and is another important intermediate for the fabrication of nuclear fuel.

The industrial fluorination of uranium dioxide into $UF_4$ involves the manipulation of hydrogen fluoride HF at high temperature. The very high toxicity of this gas requires precautions in response to environmental and safety concerns. In addition to $UF_4$, the literature mentions other examples of structures involving multidimensional (1, 2 or 3D) U(IV)-fluoride sub-networks. However, very few examples deal with isolated clusters in which U(IV) is surrounded by fluorides. So far, we have just counted one monomer ($[UF_6]^{2-}$)[3] and two different dimers ($[U_2F_{13}]^{5-}$ and $[U_2F_{14}]^{6-}$).[4,5] These numbers are very poor compared to those of the numerous molecular structures involving An(IV) and O-donor ligands.[6]

Other alternative approaches have already been proposed in the literature to synthesize new U-fluorides, leading mostly to the production of $UF_4$ or $UF_6$. For example, nitrogen trifluoride ($NF_3$) is a non-corrosive and stable gas, which has demonstrated good efficiency for the fluorination of uranium and other actinides.[7,8] Ammonium bifluoride ($NH_4HF_2$) is a stable salt melting at 126 °C. Its dissociation above 239 °C produces especially gaseous HF that can be exploited for the fluorination of actinides at a relatively low temperature.[9,10]

Thanks to their good stability, very low vapor pressure and non-volatile nature, ionic liquids (ILs) can be considered as a very safe solvent. These room-temperature molten salts have already proved their efficiency for potential applications in actinide chemistry[11] like metal extraction,[12] crystal engineering[13] and solubilization of metal oxides.[14] In the last example, the solubilization of uranium oxides is facilitated by ILs bearing a complexing chemical function (*e.g.* –COOH),[15] by the addition of nitric acid[16] or using HF-based ionic liquids.[17] On the other hand, ILs can also be used as a fluoride source and a solvent for the precipitation of fluorides.[18] In this case, the decomposition of a fluorinated anion (*e.g.* $BF_4^-$ or $PF_6^-$) liberates a fluoride anion that is able to react with a solubilized metallic cation. So far, this strategy has been established from the salts of alkali metals,[19] alkaline earth metals,[20] transition metals,[21,22] lanthanides,[23,24] and actinides,[25] which are quite soluble in ILs. In the last example involving An(IV) hexachloro complexes, the authors proposed that water could play a catalytic role in the decomposition of a hexafluorophosphate anion.

In this study, a fluorinated IL is used in a one-step reaction for the dissolution of uranium oxide and its conversion into a pure crystallized anhydrous uranium tetrafluoride (Fig. 1). This approach is validated under ionothermal reaction conditions with the transformation of $UO_2$ into $UF_4$.

---

[a] Unité de Catalyse et Chimie du Solide (UCCS), UMR CNRS 8181, Université de Lille, ENSC-Lille, Bat. C7, Avenue Mendeleïev, 59655 Villeneuve d'Ascq, France. E-mail: christophe.volkringer@ensc-lille.fr; Tel: +33 320 434 973

[b] Université de Lille, CNRS, UMR 8576, UGSF, Unité de Glycobiologie Structurale et Fonctionnelle, Lille, F-59000, France

[c] Hall de recherche de Pierrelatte, Site ORANO du Tricastin, Route du Site de Tricastin, 26701 Pierrelatte, France

[d] Synchrotron SOLEIL, L'Orme des Merisiers Saint Aubin, BP 48, F-91192 Gif sur Yvette Cedex, France

[e] CEA, CEA, DEN, DMRC, Univ Montpellier, Marcoule, France

[f] Institut Universitaire de France (IUF), 1 rue Descartes, 756231 Paris Cedex 05, France

† Electronic supplementary information (ESI) available. See DOI: 10.1039/C9DT04327F

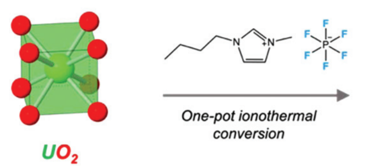

**Fig. 1** Scheme of the one-pot conversion of $UO_2$ into $UF_4$ under ionothermal conditions using the [Bmim][$PF_6$] ionic liquid both as a solvent and fluoride source.

By analogy with the industrial conversion process, we selected uranium dioxide as the metal source for the production of anhydrous uranium fluoride. The dissociation of uranium fluoride in aqueous media requires the use of a hydrophobic IL in order to avoid contact between water and the crystalline uranium-based phase.

Among various commercial fluorinated ILs, we selected 1-butyl-3-methylimidazolium hexafluorophosphate, abbreviated as [Bmim][$PF_6$]. To the best of our knowledge, [Bmim][$PF_6$] has never been exploited for the solubilization or the fluorination of metal oxides.

In this study, black powder of $UO_2$ (40 mg, 0.14 mmol) is mixed with [Bmim][$PF_6$] (2 ml) and stored in a Teflon lined reactor. Typically, when the preparation is heated below 150 °C for 24 h, we did not observe any modification. The transformation of $UO_2$ occurs in relatively short reaction times (<24 h) from 180 °C (Fig. 2). Under these conditions and for increasing contact times (Fig. S1†), we note the gradual change of the ionic liquid from colourless to brown. In parallel, the powder changes from black to green, leading to very small crystallites (<5 μm). Powder X-ray diffraction analysis indicates that this transformation is related to the conversion of black $UO_2$ into anhydrous uranium tetrafluoride $UF_4$ (Fig. 2). The solid crystallizes as a green microcrystalline powder, whatever the source of heating may be (Fig. S1†). This chemical reaction effectuated in a classic oven is quantitative after 96 h of thermal treatment, since no traces of $UO_2$ are detected in the final collected solid by powder X-ray diffraction. The same synthesis leading to pure $UF_4$ can be accelerated with a reaction time of 2 h under microwave heating (150 °C, 1200 W) (Fig. 2). The solid that crystallizes as a green microcrystalline powder under both conventional and microwave heating conditions is characterized by BET surface areas (Kr, 77 K) of 10 and 6 $m^2/\ g^{-1}$, respectively.

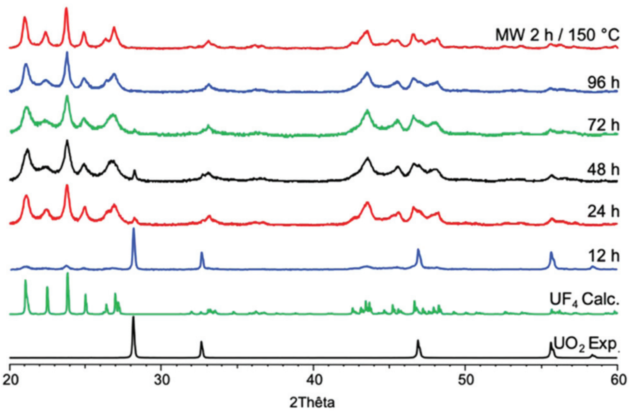

**Fig. 2** PXRD diagrams of pure $UO_2$, $UF_4$ and the solids obtained from a mixture of $UO_2$ and [Bmim][$PF_6$], heated at 180 °C in a conventional oven from 12 h to 96 h or under microwave heating for 2 hours at 150 °C.

Furthermore, inductively coupled plasma optical emission spectroscopy (ICP OES) analysis (Fig. S2†) reveals traces of uranium in solution (up to 8.6 mmol $L^{-1}$ after 96 h, conventional heating), leading to the precipitation of $UF_4$ in a yield of 89% (based on U). This very low value does not allow the identification of the uranium oxidation state by standard UV-vis spectrophotometry (Fig. S3†).

Based on these observations, we supposed that the precipitation of $UF_4$ occurs on the surface of $UO_2$ crystallites. Indeed, the amount of solid $UF_4$ increases gradually (Fig. S1†) in the medium (simultaneously with the gradual disappearance of $UO_2$) and is not preceded in solution by a peak of concentration of solubilized uranium (Fig. S3†). However, parallel to the crystallization of $UF_4$, we note a linear increase in the quantity of uranium dissolved in the IL. Such behaviour is attributed to the slow dissolution of $UF_4$ in the IL.

X-ray Photoelectron Spectroscopy (XPS) was used to characterize the oxidation state of solubilized uranium in the IL. The F 1s core level spectrum (Fig. 3(a)) confirms the presence of uranium fluoride species, as two peaks are found in the spectrum. The intense peak with binding energy (BE) 686.7 eV corresponds to the fluorophosphate contribution from the IL,[26] whereas the minor peak with BE 684.5 eV is consistent with uranium fluoride species.[27] The uranium U 4f core level spectrum shows one doublet peak, corresponding to the U $4f_{7/2}$ and U $4f_{5/2}$ half orbitals with BEs 382.2 eV and 393.0 eV respectively and a full width at half maximum (FWHM) of 1.5 eV (Fig. 3(b)). An intense peak localized at 402.1 eV is also

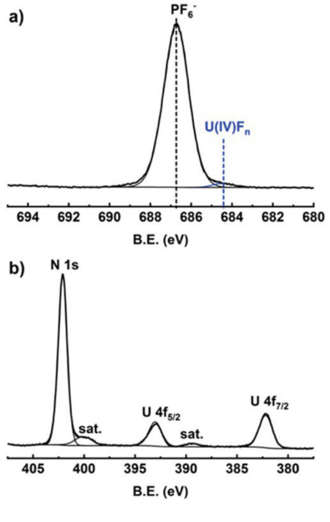

**Fig. 3** XPS F 1s core level spectra (a) and N 1s core level spectra (b) of the $UF_4$ synthesised supernatant (180 °C, 24 h).

present in the spectrum and corresponds to the N 1s orbital from the imidazolium species in the IL. In addition, two minor peaks with BEs 389.3 eV and 400.1 eV are found in the U 4f spectrum. These peaks correspond to the U $4f_{7/2}$ and U $4f_{5/2}$ satellite orbitals respectively, and are due to the shake-up or charge transfer processes.[27,28] The satellite-primary U $4f_{7/2}$ peak binding energy separation is equal to 7.1 eV and the satellite/primary U $4f_{7/2}$ peak intensity ratio is equal to 0.11. The high U $4f_{7/2}$ BE, alongside the satellite-primary BE separation and intensity ratio, is consistent with the presence of uranium fluoride species with a 4+ oxidation state.[27,29] Besides, the presence of the $U^{5+}$ species can be ruled out, as the U $4f_{7/2}$ peak from $UF_5$ presents a large FWHM and almost no satellite peak.

In order to investigate the modification that is associated with the ionic liquid, the solution was also analysed by solution-state NMR spectroscopy. The $^{13}C$ NMR signature of the supernatant previously treated at 180 °C for 24 h is comparable to that of the unreacted IL, proving that the organic cation is not decomposed during the reaction (Fig. S6†). Only a minor difference is observed in the ionic liquid containing uranium, which exhibits a small peak broadening due to the presence of paramagnetic U(IV) in solution. On the other hand, $^{19}F$ and $^{31}P$ NMR results confirm that the hexafluorophosphate anion $PF_6^-$ from [Bmim][$PF_6$] is more fragile under the reaction conditions. After the thermal treatment (24 h, 180 °C), the initial heptet at $\delta(^{31}P) = -144.3$ ppm ($^1J_{PF} = 711$ Hz) is partially transformed to a triplet $\delta(^{31}P) = -17.6$ ppm ($^1J_{PF} = 953$ Hz), whereas the $^{19}F$ signature presents a doublet in both cases centred at $\delta(^{19}F) = 71.7$ ppm ($^1J_{PF} = 710$ Hz) which shifts to $\delta(^{19}F) = 83.4$ ppm ($^1J_{PF} = 954$ Hz) at the end of the reaction (Fig. 3).

These new signals are consistent with the existence of the $PO_2F_2^-$ anion,[30] a known hydrolysis product of $PF_6^-$ according to eqn (1). $PO_2F_2^-$ is accompanied by the production of hydrofluoric acid. The initiation of $PF_6^-$ hydrolysis is guaranteed by the traces of water in the initial IL (1 mmol $L^{-1}$) and self-propagated by the generation of water during $UF_4$ formation (eqn (2)). This mechanism, clearly proved by NMR analysis, is different from the process usually supposed for the fluorination of cations and based on the decomposition of $PF_6^-$ into gaseous phosphorus pentafluoride ($PF_5$) and a fluoride anion ($F^-$).[19]

$$PF_6^- + 2H_2O \rightarrow PO_2F_2^- + 4HF \tag{1}$$

$$UO_2 + 4HF \rightarrow UF_4 + 2H_2O \tag{2}$$

Based on the peak intensity (Fig. S4†), the quantity of $PO_2F_2^-$ remains in a minority in solution, compared to the original $PF_6^-$ anion. Whereas this reaction induces the appearance of HF, the whole process remains very safe. Indeed, the quantity of this species must remain very low due to its consummation in a reaction cycle requiring its disappearance (eqn (1) and (2)).

The different NMR spectra ($^{13}C$, $^{19}F$, and $^{31}P$) do not show other peaks that could correspond to the other hydrolysis products and solubilized U(VI) complexes. Therefore, the NMR technique is not adapted for the detection of U(IV) complexes due to the paramagnetic character of this cation (Fig. 4).

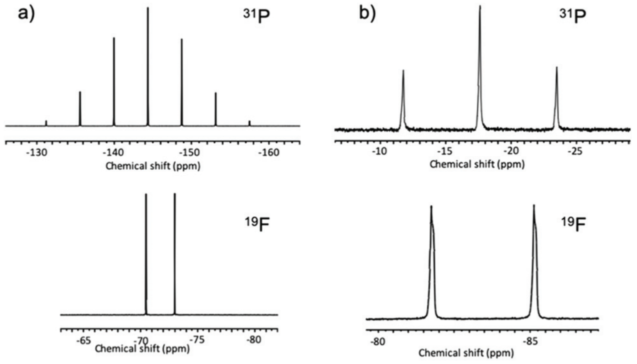

**Fig. 4** $^{19}F$ (at 7.0 T) and $^{31}P$ (at 9.4 T) NMR spectra recorded at 303 K of neat [Bmim][$PF_6$] (a) and the supernatant collected after a reaction of 24 h at 180 °C in a conventional oven (b).

The characterization of the supernatant isolated from the precipitation of $UF_4$ (180 °C, 24 h) was completed by X-ray absorption Spectroscopy (XAS). XAS measurements of the sample were performed at the U-$L_3$ edge. The shape of the XANES spectrum (Fig. S7†) is typical of the signature of tetravalent uranium in solution. The XANES region has a maximum (white line) at 17180.8 eV and does not show a shoulder on the right side of the line, typical of the uranium(VI) samples.[31] Therefore, the EXAFS and the corresponding Fourier transform (FT), as well as the associated fits, are shown in Fig. 5. One can see qualitatively that the signal is dominated by a single contribution and this is reflected in the FT by a main peak with a maximum at 1.65 Å. By fitting the signal in the *R* space with a single fluorine contribution, it is possible to achieve a good fit with a U–F distance of 2.06 Å and compatible with five neighbouring atoms like in the $UF_5^-$ anion. The results are given in Table S1.† Moreover, these distances are in good agreement

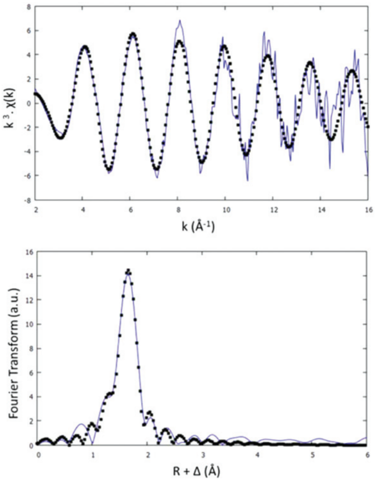

**Fig. 5** U-$L_3$ edge $k^3$-weighted EXAFS (top) and the corresponding Fourier transform (bottom) of the supernatant sample. The blue lines represent the experimental spectra and the dots represent the fits.

with those already reported for other U(IV) and U(V) fluorides.[3,32] The existence of $UF_5^-$ seems to be counterintuitive due to the very large size of the U(IV) cation, which is used to adopt coordination numbers greater than or equal to 6. However, it has to be noted that penta-coordinated uranium was already mentioned in different complexes.[33,34] The stabilization of $UF_5^-$ in [Bmim][$PF_6$] can be explained by the very low concentration of this species and $H_2O$, limiting the hydrolysis and/or the condensation of the inorganic anion. Furthermore, an effect from the IL cannot be ruled out.

As mentioned above, the appearance of $UF_5^-$ is correlated to the crystallization of $UF_4$. This phenomena can be interpreted as the slow dissolution of $UF_4$ in the IL, according to eqn (3)

$$UF_4 + F^- \rightarrow UF_5^- \quad (3)$$

In conclusion, we have demonstrated for the first time the direct conversion of $UO_2$ to $UF_4$ under ionothermal reaction conditions. The chemical mechanism is based on a one pot reaction process in which a fluorinated ionic liquid plays the dual role of solvent and fluoride source. $^{19}F$ and $^{31}P$ NMR analyses indicate that the catalytic mechanism of fluorination starts from the hydrolysis of the $PF_6^-$ anions and generates HF, which is immediately consumed for the fluorination of uranium. The decomposition of $PF_6^-$ in the presence of water and the metallic cation is also accompanied by the production of $PO_2F_2^-$. $H_2O$ appears as the driving force of the conversion of $UO_2$ to $UF_4$, since the hydrolysis of $PF_6^-$ requires water molecules produced by the reaction between HF and $UO_2$. The initial hydrolysis of $PF_6^-$ is permitted by the traces of water in the initial IL. EXAFS/XANES and XPS spectroscopy analyses indicate that the precipitation of $UF_4$ is followed by its slow dissolution as the $UF_5^-$ anion.

This new approach for the synthesis of $UF_4$ is considered as an interesting and very safe alternative for the usual industrial process requiring high temperature and a large amount of HF. Furthermore, it opens up new methods for the stabilization and the synthesis of molecular U(IV)-fluorides, which can serve as a building unit for the production of new fluorinated materials.

## Conflicts of interest

There are no conflicts to declare.

## Acknowledgements

The authors would like to thank Nora Djelal, Laurence Burylo and Philippe Devaux for their technical assistance with the SEM image and powder XRD analysis. The Institut Universitaire de France (IUF), Chevreul Institute (FR2638), Fonds Européen de Développement Régional(FEDER), CNRS, Région Nord Pas-de-Calais and Ministère de l'Education Nationale de l'Enseignement Supérieur et de la Recherche are acknowledged for funding this work. Dr F. Joly also thanks University of Lille and ORANO for his PhD fellowship.

## Notes and references

1 C. R. Edwards and A. J. Oliver, *JOM*, 2000, **52**, 12–20.

2 B. Morel and B. Duperret, *J. Fluorine Chem.*, 2009, **130**, 7–10.

3 K. S. Pedersen, K. R. Meihaus, A. Rogalev, F. Wilhelm, D. Aravena, M. Amoza, E. Ruiz, J. R. Long, J. Bendix and R. Clerac, *Angew. Chem., Int. Ed.*, 2019, **58**, 15650–15654.

4 R. J. Francis, P. S. Halasyamani, J. S. Bee and D. O'Hare, *J. Am. Chem. Soc.*, 1999, **121**, 1609–1610.

5 Y. L. Lai, R. K. Chiang, K. H. Lii and S. L. Wang, *Chem. Mater.*, 2008, **20**, 523–530.

6 K. E. Knope and L. Soderholm, *Chem. Rev.*, 2013, **113**, 944–994.

7 A. M. Casella, R. D. Scheele and B. K. McNamara, *AIP Adv.*, 2015, **5**, 127230.

8 B. McNamara, R. Scheele, A. Kozelisky and M. Edwards, *J. Nucl. Mater.*, 2009, **394**, 166–173.

9 J. B. S. Neto, E. F. U. de Carvalho, R. H. L. Garcia, A. M. Saliba-Silva, H. G. Riella and M. Durazzo, *Nucl. Eng. Technol.*, 2017, **49**, 1711–1716.

10 B. Claux, O. Benes, E. Capelli, P. Soucek and R. Meier, *J. Fluorine Chem.*, 2016, **183**, 10–13.

11 K. Takao, T. J. Bell and Y. Ikeda, *Inorg. Chem.*, 2013, **52**, 3459–3472.

12 X. Q. Sun, H. M. Luo and S. Dai, *Chem. Rev.*, 2012, **112**, 2100–2128.

13 A.-V. Mudring and S. Tang, *Eur. J. Inorg. Chem.*, 2010, 2569–2581.

14 K. Binnemans, *Chem. Rev.*, 2007, **107**, 2592–2614.

15 C. J. Rao, K. A. Venkatesan, K. Nagarajan and T. G. Srinivasan, *Radiochim. Acta*, 2008, **96**, 403–409.

16 I. Billard, C. Gaillard and C. Hennig, *Dalton Trans.*, 2007, 4214–4221.

17 C. A. Zarzana, G. S. Groenewold, M. T. Benson, J. E. Delmore, T. Tsuda and R. Hagiwara, *J. Am. Soc. Mass Spectrom.*, 2018, **29**, 1963–1970.

18 A. B. Pereiro, J. M. M. Araujo, S. Martinho, F. Alves, S. Nunes, A. Matias, C. M. M. Duarte, L. P. N. Rebelo and I. M. Marrucho, *ACS Sustainable Chem. Eng.*, 2013, **1**, 427–439.

19 J. Olchowka, M. Suta and C. Wickleder, *Chem. – Eur. J.*, 2017, **23**, 12092–12095.

20 J. S. Xu and Y. J. Zhu, *CrystEngComm*, 2012, **14**, 2630–2634.

21 D. S. Jacob, L. Bitton, J. Grinblat, I. Felner, Y. Koltypin and A. Gedanken, *Chem. Mater.*, 2006, **18**, 3162–3168.

22 C. L. Li, L. Gu, S. Tsukimoto, P. A. van Aken and J. Maier, *Adv. Mater.*, 2010, **22**, 3650–3654.

23 C. Zhang, J. Chen, Y. C. Zhou and D. Q. Li, *J. Phys. Chem. C*, 2008, **112**, 10083–10088.

24 D. S. Zhang, T. T. Yan, H. R. Li and L. Y. Shi, *Microporous Mesoporous Mater.*, 2011, **141**, 110–118.

25 S. I. Nikitenko, C. Berthon and P. Moisy, *C. R. Chim.*, 2007, **10**, 1122–1127.

26 I. J. Villar-Garcia, E. F. Smith, A. W. Taylor, F. L. Qiu, K. R. J. Lovelock, R. G. Jones and P. Licence, *Phys. Chem. Chem. Phys.*, 2011, **13**, 2797–2808.

27 E. Thibaut, J. P. Boutique, J. J. Verbist, J. C. Levet and H. Noel, *J. Am. Chem. Soc.*, 1982, **104**, 5266–5273.

28 T. Gouder, R. Eloirdi and R. Caciuffo, *Sci. Rep.*, 2018, **8**, 1–7.

29 E. S. Ilton and P. S. Bagus, *Surf. Interface Anal.*, 2011, **43**, 1549–1560.

30 E. N. Keyzer, P. D. Matthews, Z. G. Liu, A. D. Bond, C. P. Grey and D. S. Wright, *Chem. Commun.*, 2017, **53**, 4573–4576.

31 C. Hennig, A. Ikeda-Ohno, F. Emmerling, W. Kraus and G. Bernhard, *Dalton Trans.*, 2010, **39**, 3744–3750.

32 C. G. Gianopoulos, V. V. Zhurov, S. G. Minasian, E. R. Batista, C. Jelsch and A. A. Pinkerton, *Inorg. Chem.*, 2017, **56**, 1775–1778.

33 C. J. Burns, D. L. Clark, R. J. Donohoe, P. B. Duval, B. L. Scott and C. D. Tait, *Inorg. Chem.*, 2000, **39**, 5464–5468.

34 C. A. P. Goodwin, F. Tuna, E. J. L. McInnes, S. T. Liddle, J. McMaster, I. J. Vitorica-Yrezabal and D. P. Mills, *Chem. – Eur. J.*, 2014, **20**, 14579–14583.